A Numerical Simulation of Jet Breakup in Melt Coolant Interactions

Sachin Thakre, Louis Manickam, Weimin Ma

Division of Nuclear Power Safety, Royal Institute of Technology (KTH),
AlbaNova University Center, Roslagstullsbacken 21, 106 91 Stockholm, Sweden
thakre@safety.sci.kth.se, louis@safety.sci.kth.se, ma@safety.sci.kth.se
Phone: +46 8 5537 8821 Fax: +46 8 5537 8830

ABSTRACT

During a hypothetical severe accident of a light water reactor (LWR), molten corium could fall in the form of jet into a water pool. The jet fragmentation is crucial process during fuel coolant interactions (FCI) which fragment into droplets and disperse in the coolant, and it may cause a steam explosion. This paper deals with a study of computational fluid dynamics on the melt jet falling into a water pool in order to get qualitative and quantitative understanding of initial premixing phase of FCI. The preliminary objectives to pursue are modeling of jet fragmentation and estimation of the jet breakup length. A commercial CFD code ANSYS FLUENT 14.0 is used for the 2D numerical analysis employing Volume Of Fluid (VOF) method. The problem and simulation conditions are similar to the jet breakup tests carried out at KTH (Manickam et al., 2014). Initially, a fragmentation/breakup pattern of the jet is discussed. Further, the effect of jet diameter and the jet injection velocity on the jet breakup length is studied, with a wide range of ambient Weber number (We_a) from 1.25 to 1280. The numerical results compared with the experimental data are in a reasonable agreement. The impacts of physical properties of melt (density, viscosity and surface tension) on the jet breakup lengths are also investigated and presented. Finally the droplet size distributions are obtained based on the simulation results. These preliminary data may be helpful to substantiate the understanding of the phenomena during melt jet interactions with coolant.

KEYWORDS:

Fuel-coolant interactions, melt jet instability melt jet fragmentation, jet breakup length.

1. INTRODUCTION

During a hypothetical nuclear severe accident in light water reactors, a molten corium from fuel core region may get in contact with the water pool. It may either fall into the water in

lower plenum from the initial core region (in-vessel case) or into the lower cavity of containment (ex-vessel case). It has been hypothesized that the melt will pour in the form of jets. A steam explosion may occur as a result of melt-coolant interactions. During in-vessel case, the core melt may relocate at the bottom of reactor pressure vessel (RPV) in the form of smaller size multiple jets (molten part may drain through the openings from the degraded core), where it will interact with water and may cause steam explosion. However, the melt will settle at the bottom and affect the bottom of pressure vessel if not coolable. Ex-vessel fuel-coolant interactions (FCI) phenomena are possible during the severe accident of some of the LWRs, such as Nordic BWRs, where RPV may fail near the bottom due to heating from non-coolable molten melt. Moreover, cavity flooding technique is employed by the Nordic BWRs as a severe accident management strategy. Therefore, for such conditions, the melt may fall into a water pool after breaching the RPV, creating the chances of steam explosion. The release of melt may be gravity driven or at higher velocity, depending on the pressure inside RPV. In case of BWRs, the size of jet may be of CRGTs (control rod guide tube) and IGTs (instrument guide tubes) in case of its failure or a large break size. Severity of steam explosion can be decided by the quantity of melt participation in a water pool and by the limited breakup of the molten pour stream flowing through the water prior to steam explosion (Ginsberg, 1985).

The modes and regimes of liquid jet breakup into water are decisive for the intermixing of melt and water, and therefore it forms the initial conditions for steam explosion energetics, quenching of melt and pressurization of the system through vapor generation. There are several regimes of jet breakup mentioned in Ginsberg (1985); laminar, transition, turbulent and atomization, which vary according to increasing jet injection velocity. The breakup lengths and the transition between regimes are quantified in terms of Weber and Reynolds' numbers. Bürger et al. (1995) used Ambient Weber number ($We_a=\rho_l V^2 D/\sigma$) for jet breakup study, where density (ρ_l) is of ambient liquid: V, D and σ are velocity, jet diameter and surface tension respectively. Influence of surface tension is dominant at lower injection velocities whereas the jet enters into an atomization regime at higher velocities, characterized by the spray production due to intensive stripping of very small size particles from the jet surface. Two types of instabilities to describe the jet breakup are mentioned in the literature: Taylor instability and Kelvin-Helmholtz instability (KH). Taylor instability may occur at the leading edge due to deceleration of the jet in surrounding medium (Bürger et al., 1995). After the jet enters into water, there is continuous stripping from the jet surface which causes the thinning

of jet and finally the coarse breakup of a coherent core may occur. This coarse breakup of liquid core into relatively large droplets may also be followed by a subsequent secondary breakup where the bigger droplets further breaks into smaller fragments (Wang et al., 1989).

Melt jet fragmentation, modes of breakup and jet-breakup length has been studied previously by many investigators, experimentally and numerically (Bürger et al., 1995; Wang et al., 1989; Berg et al., 1993; Nishimura et al., 1999; Bang et al., 2003). Despite of many experiments and numerical work done on liquid-liquid systems, it has not yielded to a sufficient understanding of the fragmentation process. Due to complexity of the phenomena during intermixing of the jet with water, it makes difficult to understand the several mechanisms simultaneously. However, it can be worthwhile to study the melt jets fragmentation at lower temperature which can help to analyze the separate phenomena (hydrodynamic fragmentation in non-boiling) and understand the mechanism by standalone method. It can also be helpful for model development and validation. There are some experiments performed using the jets of low-melting Wood's metal in water (Spencer et al., 1986), having non-boiling conditions.

In the present work, a two dimensional numerical analysis of melt jet fragmentation/breakup has been carried out using a commercial CFD code, ANSYS FLUENT 14.0. The numerical work is motivated with experimental investigation of melt jet breakup experiments carried out at Royal Institute of Technology (KTH), Sweden (Manickam et al., 2014). Wood's metal is used as a jet interacting with water, without film boiling. The two phase calculations employ Volume of Fluid method (VOF) where the phases are treated immiscible. The present analysis includes the pattern of jet fragmentation which is followed by the study of effect of jet diameter, jet velocity on the jet breakup length. It is then extended to study the effect of melt physical properties on the jet breakup length followed by characterization of droplet size distribution in the premixing region.

2. NUMERICAL METHODOLOGY

VOF method is available in FLUENT code under the multi-phase calculation module (ANSYS FLUENT 14.0 manual). A VOF method is a mathematical model used for tracking fluid-fluid non-penetrating interfaces. In each control volume the sum of volume fractions of all phases is unity. A unit value of volume fraction would correspond to a cell of that fluid and a zero value would indicate no fluid. And, the volume fraction between zero and one must contain an interface. Among the two phases, water is a primary phase and the melt is secondary phase. Due

to assumption of isothermal conditions, energy equation is not used in the present calculations. It is known that, at lower velocities, initially the jet deforms linearly and may be considered to undergo axisymmetric deformation. Although the jet may not possess symmetry after jet starts destabilization as seen in experiments, the 2D simulations can still capture some extent of the instability and breakup phenomena, while keeping computationally affordable. The below comparisons of the numerical results with the experimental data (Manickam et al., 2014) also prove the validity of the simulations. Therefore, in this study the 2D domain is considered for analysis as shown in Fig. 1a. There is an inlet for melt jet at the top of the domain. Two sides and the bottom boundary are treated as walls whereas at the top surface, pressure is specified. The continuous jet is initialized with specific velocity. A comparatively bigger domain is used for 20 mm jet diameter in order to accommodate the whole jet breakup phenomena. The details of a geometry are used same as test section of experimental facility employed for jet fragmentation study. A structured mesh is used which is done by the ICEMCFD meshing software. A melt jet is initialized using the user defined functions (UDF), a routine in FLUENT which can be dynamically linked and programmed by the user.

A non-Iterative Time Advancement (NITA) technique is employed for optimizing the computational time and efforts, reducing the large number of outer iteration required in iterative time advancement techniques. An explicit time marching scheme has been used for the volume fraction calculations. Pressure-Implicit with Splitting Operators (PISO) scheme is employed for pressure-velocity coupling, and a Geo-Reconstruct scheme is used for interface reconstruction calculations (details can be found in ANSYS FLUENT 14.0 user manual). Surface tension at the interface (to be used as a source term in a momentum equation for VOF calculations) is calculated by the Continuum Surface Force (CSF) model by Brackbill et al. (1992) implemented in ANSYS FLUENT 14.0 code. Properties of Wood's metal are specified to the secondary liquid (melt jet) in simulations, which are given in Table 1.

In order maintain a consistency with best practice guidelines for CFD in nuclear power safety (Mahaffy, 2010), a consideration is given to selection of appropriate physical model and reducing the numerical issues including creation of suitable spatial grid. Moreover, the mesh quality study is carried out to enhance the accuracy of the solution. Time step sensitivity for this transient analysis is monitored using Courant number (Co) and it is maintained as Co=0.25 for all the calculations. A Lenovo work station with 4 GB RAM, Intel and Xeon processors of 2.4 GHz each, is used for the numerical simulations. The calculations are carried out till the jet

breakup observed. The CPU time taken by calculations varied according to the conditions used in the calculations such as jet diameter, jet velocity, etc. The some calculations took almost a week to complete, and the longest calculation took almost 9 days of CPU time.

2.1 Mesh Quality Study

In order to accurately capture the interfaces in two phase flow systems, the adaptive mesh refinement scheme is efficient, which, the authors have successfully used in their earlier studies (Thakre et al., 2013; Thakre and Ma, 2015). Therefore adaptive refinement (as shown in Fig. 1b) is applied in the present study since an accurate prediction of the interfaces is required particularly during large deformations, breakup/fragmentation of jet. This technique also saves the computational time since the grid refinement is done only at specific locations.

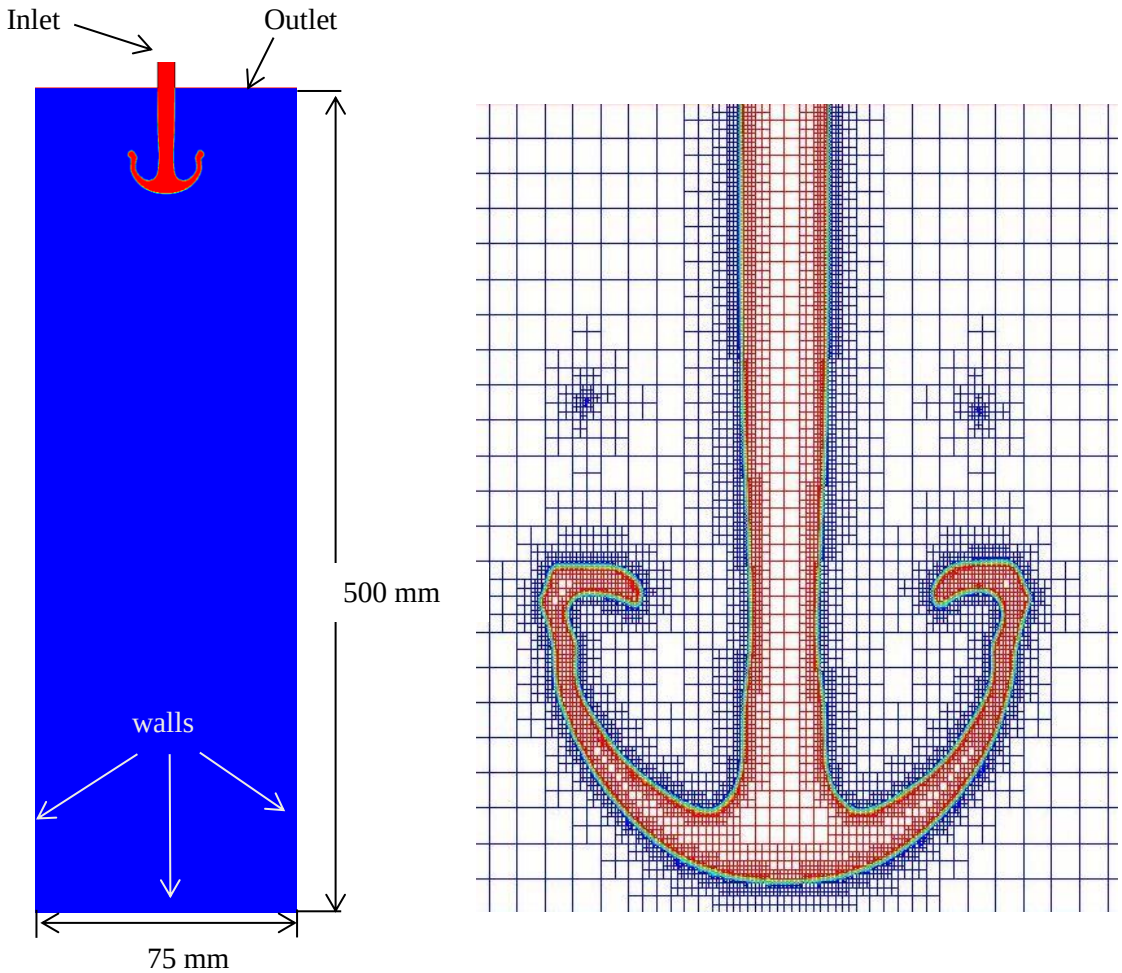

Fig. 1: (a) Geometry details and boundary conditions, (b) mesh adaption.

Moreover, the quality of mesh is assessed by analyzing the results of the calculations carried out at various levels of mesh refinement at the interfaces. Three different cases are compared for the

present study, as shown in Fig. 2, where, the term Δx represent the dimensions of the finest cell used during calculations. Considering the accuracy in predicting the interfaces and the total calculation time, the optimum mesh having dimensions Δx=0.1×125 mm is used for the present calculations.

Table 1: Properties of Wood's metal.

Material	Surface tension (*N/m*)	Density (kg/m^3)	Viscosity (*Pa.s*)
Wood's metal	1	9700	0.00194

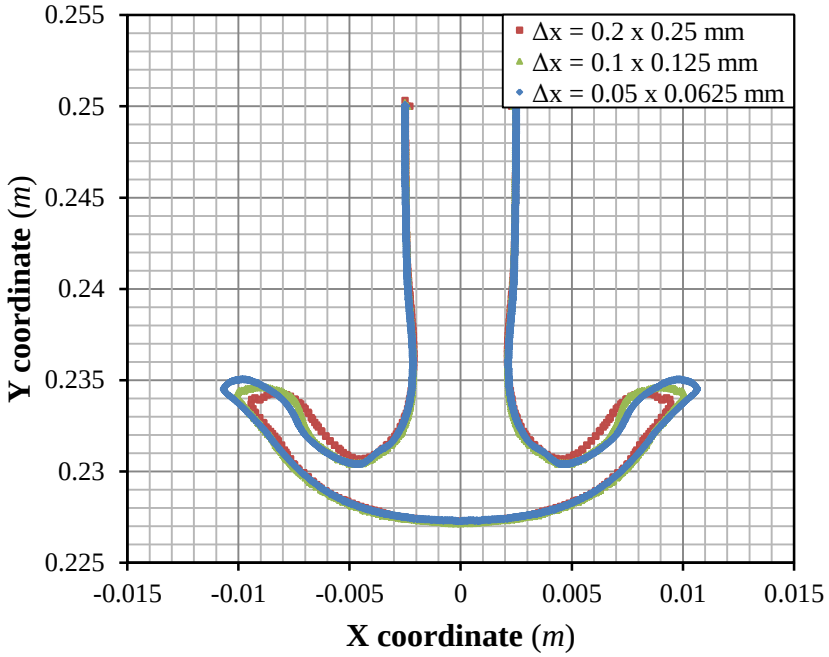

Fig. 2: Jet-coolant interface plot (D_j=5 *mm*; V_j=1.5 *m/s*).

3. RESULTS AND DISCUSSIONS

3.1 Jet Breakup Pattern

The melt jet falling into a coolant may undergo various types of breakup quantitatively depending on the factors such as jet velocity or relative velocity between jet-coolant, and jet diameter. The phenomena involved in the process of jet breakup are instabilities at the leading edge and on the jet surface parallel to flow. The dominance of these phenomena depends on the relative velocity (jet-coolant) though it may have a combined effect on the jet breakup. At lower jet velocities, generally the jet surface tends to remain intact due to dominance of surface tension effect. However, the jet deforms at the leading edge due to deceleration forces (as shown in Fig. 3a) and starts stripping in the form of ligaments which further breaks into droplets (it may be treated as a coarse breakup). At some jet velocities, the leading edge

deforms into a mushroom-like shape which starts releasing ligaments from its periphery. These leading edge instabilities are recognized as Taylor instabilities whose occurrence depends on the strong enough deceleration forces (Bürger et al., 1995).

At higher jet velocities, the relative flow parallel to the jet surface overcomes the surface tension effect and leads to stripping of droplets. These stripping from the jet surface can be of the form of Kelvin-Helmholtz instability (Fig. 3b) which further causes the thinning of jet.

Fig. 3 shows the volume fraction contours (at different time intervals) of the Woods metal jet at various Weber numbers. Ambient Weber number (We_a) used in this study is to maintain the similar terminology of earlier researchers which makes easier for data comparison. There are several jet breakup regimes identified with increasing injection velocities or Weber number (Ginsberg, 1985; Bürger et al., 1995). It varies from surface tension influenced axisymmetric regime at lower velocities to atomization zone/severe fragmentation at higher velocities. Fig. 3a is an example of jet deformation and breakup at lower velocity/Weber number, where the jet is mostly axisymmetric in the beginning and deforms at the leading edge, with no instability on the surface in tangential direction. It undergoes sinusoidal destabilization after achieving some length and its growth leads to the jet breakup. The droplets are of bigger size and mainly stripped from the leading edge. The jet breakup pattern shown in Fig. 3b is at moderate Weber number which has, in addition to leading edge deformation, a stripping in tangential direction at the jet surface. This is mainly the K-H instability which grows further downwards and causes thinning of jet. It is then followed by the instability in the transverse direction (Rayleigh-Taylor instability type), due to which, the jet cross-section starts decreasing at many places and the jet forms small segments joined to each other by a small ligament. After a further growth in instability, finally a jet breakup occurs at one of the small cross-sectional areas.

The case shown in Fig. 3c is jet breakup in atomization regime where severe stripping occurs from the jet surface parallel to the flow. Due to shorter wavelength of K-H instabilities the sizes of the fragmented droplets are very small and the area around the jet is occupied by the cloud of the fine fragments. The destabilization of the jet occurs at early stage and therefore has a shorter breakup length. From the above described three cases, it is seen that the size of the fragmented droplets gets smaller with increasing Weber number and also increase in the amount of fragmented mass due to excessive stripping from the jet surface. However, in most

of the regimes, during breakup, the jet breaks into bigger droplets of ligaments shape which further undergoes secondary fragmentation.

Moreover, a leading edge of the jet deforms initially into a shape similar to dome or an inverted Mushroom. Similar type of Mushroom-like shape has also been observed by some researchers (Dinh et al., 1999) in their low velocity small diameter water-paraffin oil experiments. In the present analysis, a jet breakup length is taken as a length of a coherent jet similar to the terminology used in Bürger et al. (1995).

Similar type of jet fragmentation/breakup pattern can be observed in snapshots of Fig. 4 from the experiments conducted at KTH (carried out with Wood's metal as a jet in water). Fig. 4a shows the jet with lower injection velocity, where there is no sideways stripping on the jet surface. However, the jet is deformed near the leading edge may be due to the deceleration forces as mentioned earlier in the text. Moreover, the fragmentation occurs near the leading edge but not from the sides of the jet, which is clear from both experimental and simulations cases. In Fig. 4b, there is significant stripping from the side surface of jet (in addition to fragmentation at leading edge) to form a cloud of particles around the jet surface. As mentioned earlier, it is due to the K-H instability which occurs at higher Weber number. Such case makes it difficult to visualize the breakup in experimental conditions.

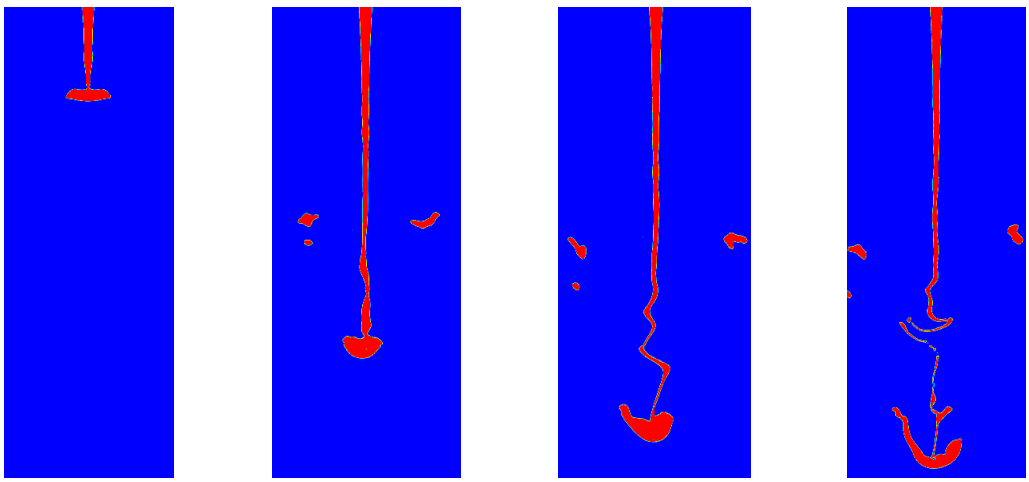

(I) (II) (III) (IV)

a) $We_a = 1.25$; $D_j = 5$ mm; $V_j = 0.5$ m/s

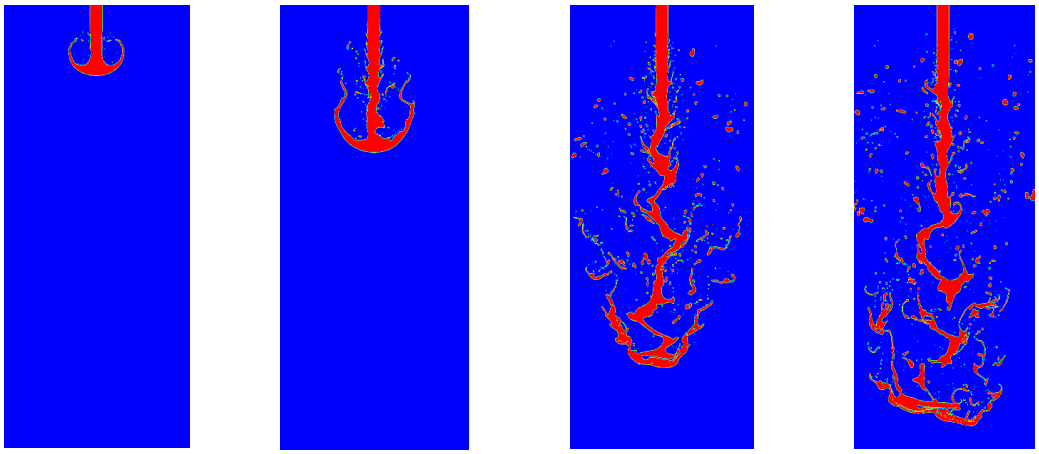

(I) (II) (III) (IV)

b) $We_a = 125$; $D_j = 5$ mm; $V_j = 5$ m/s

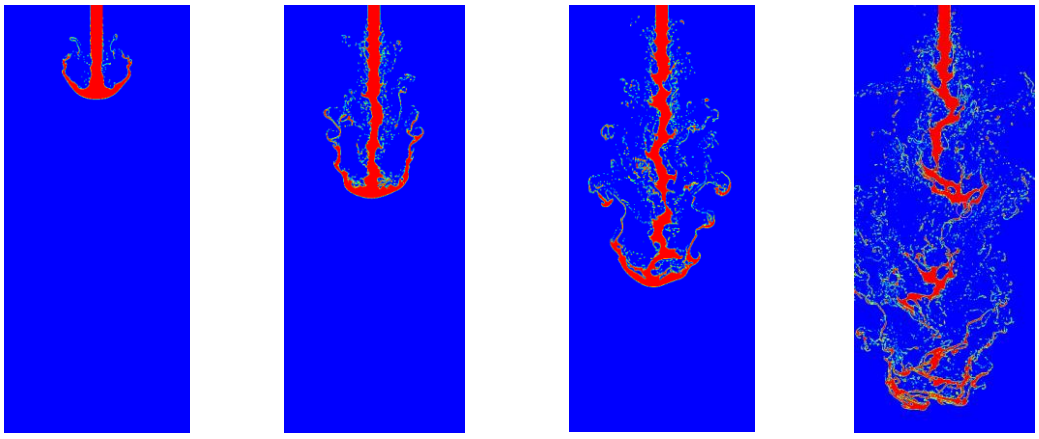

(I) (II) (III) (IV)

c) $We_a = 1280$; $D_j = 5$ mm; $V_j = 16$ m/s

Fig. 3 Jet deformation and breakup while progression in a water pool.

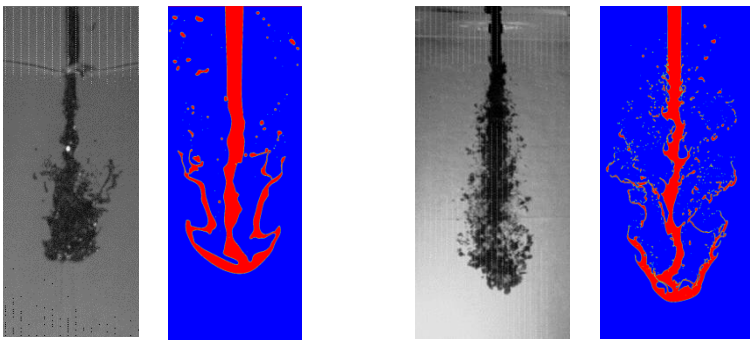

(a) $We_a = 14.4$; $D_j = 10$ mm; $V_j = 1.2$ m/s (b) $We_a = 192$; $D_j = 20$ mm; $V_j = 3.08$ m/s

Fig. 4: Snapshots of jet deformation and breakup from experiments at KTH.

3.2 Jet Breakup Length

It is well known from the above description that the melt jet breaks at some length while falling into the coolant. The first instance when the jet detaches from its leading part can be considered

as a breakup and the coherent part can be considered as a jet breakup length. During experimental conditions, a coherent jet can be clearly seen at lower velocities. However, it forms a cloud of particles at higher jet velocities (Fig. 4b) and the coherent jet is not clearly visible, which makes it quite challenging to recognize the jet breakup and the breakup length. During many experimental investigations, the leading edge advance is plotted with the time. It is found that there is a decrease in velocity of the leading edge after some distance, and this length is considered as a jet breakup length. Moreover, the length may not remain constant after first breakup, but has a transient nature. Some simulations are carried out to see the transient of breakup length which are shown in Fig. 5 as the variation in the jet breakup length with time. Three cases with different velocities show the jet breakup length varies following a specific pattern. It is found that initially a coherent jet length increases with the time to some extent, which then breaks somewhere near leading edge. It again increases, and this way the process continues in periodic intervals. During a jet progression into a pool, instability starts developing on the jet surface which maximize near leading edge. At some instance (may be termed as threshold) the instability intensifies and again breaks the jet. Therefore instability on the jet surface may be responsible for the variation in the jet breakup length.

During the present study, a coherent jet length just after first breakup is considered as a jet breakup length. There are the possible effects of various parameters of jet including material properties on the jet breakup length which are studied and presented in the following sections.

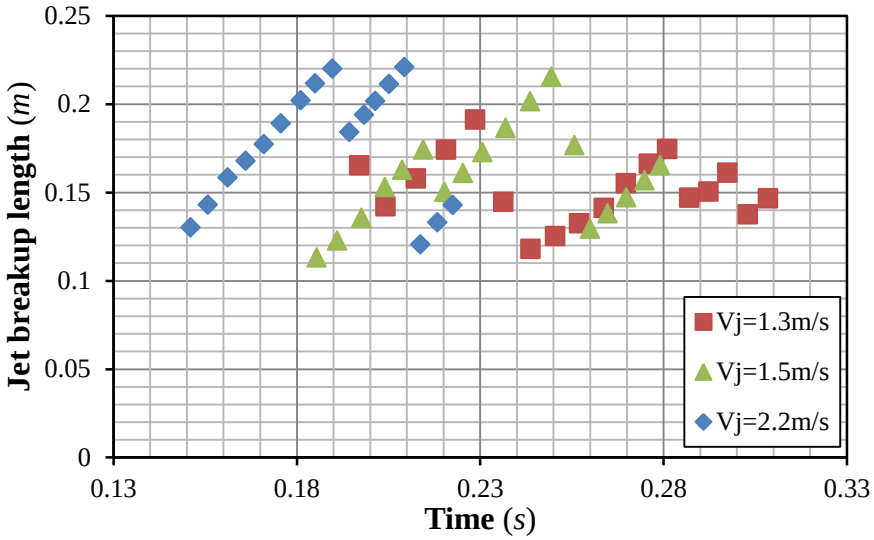

Fig. 5: Dynamics of the jet breakup for different velocities (D_j=5 *mm*).

3.2.1 Effect of Jet Diameter

The variation in the breakup mechanism of jet fragmentation may appear due to diameter effect. Significantly larger diameter may strongly increase Weber number (We_a) which may support atomization, i.e. an increased contribution of stripping from the jet surface (Bürger et al., 1995). However the jet diameters considered in the present calculations are at smaller scale.

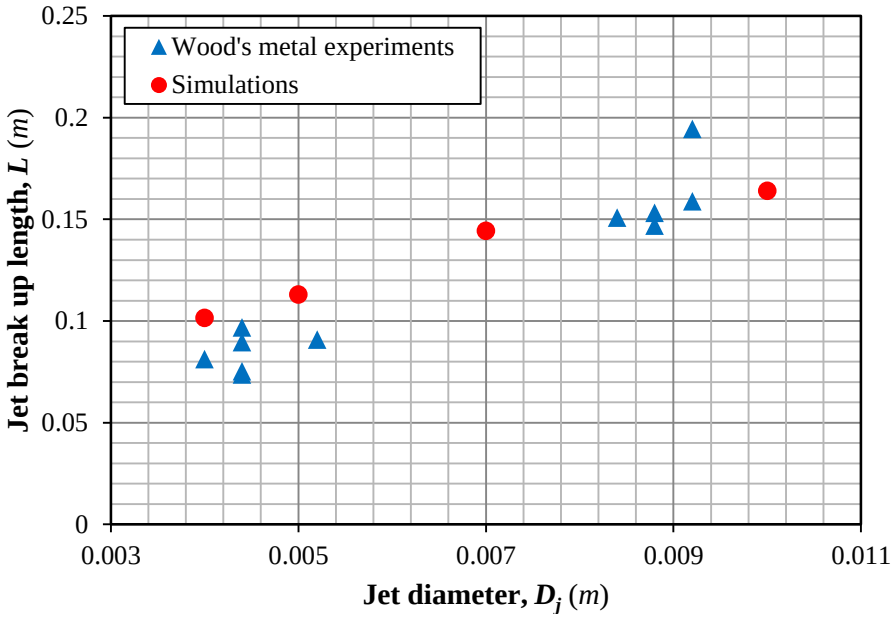

Fig. 6: Variation of jet breakup length with respect to jet diameter (V_j=1.5 *m/s*).

In order to understand the effect of jet diameter (D_j) on the jet breakup length (L), simulations with different diameter sizes are carried out. Fig. 6 shows the variation in jet breakup length (L) with a size of melt jet. It illustrates the breakup length increases with increase in the jet diameter. The data from Wood's metal experiments at KTH is used for comparison. In the experiments, the jet diameter is measured at the time when jet is about to enter into water pool. Moreover, the jet velocities measured at the same instant is in the range of 1.4-1.7 m/s recorded after test repetitions. It significantly varies the absolute percentage in Weber number. It can be noted from Fig. 9, at lower We_a (1-30), the jet breakup length can have significant variation. Therefore, such variation in jet breakup length for a same jet diameter, in experiments can be plausible, as shown in Fig. 6. The comparison between simulation results and experimental data shows some overestimation by the simulations for smaller diameters, though it less than 25%. This overestimation of the values may be comprehended by the limitations of two dimensional analyses.

It is known that the jet fragmentation/breakup primarily involves two mechanisms: sideways stripping and the coarse breakup. The sideways stripping causes the thinning of a jet and it leads to a coarse breakup near leading edge, where the jet breaks into multiple small segments (as discussed in earlier section). It may be understandable that the dimensional jet breakup length is higher for bigger diameter. For bigger jets, more surface area is available for sideways stripping which gives more droplets around the jet. If the dimensionless quantity is taken into account, the Weber number increases with jet diameter in a direct proportion. Therefore more stripping at higher We_a also satisfies the criteria. The coarse breakup occurring near the leading edge may happen earlier for bigger diameter, even before enough thinning of the jet due to stripping. It may be the possible reason for the decrease in *L/D* ratio with a rise in diameter, in the present analysis. However the possibility may not be avoided that the trend will not be similar for big scale jets.

3.2.2 Effect of Jet Velocity

As mentioned earlier and shown, different regimes of jet behaviors can be identified with increasing injection velocity. Since the Weber number is directly proportional to the square of the relative velocity between jet and coolant, it is strongly increased by change in velocity. Some experiments with 20 mm jet diameter are carried out on a large scale jet breakup facility at KTH. There is small variation in the jet injection velocities among the conducted tests. The simulations are carried out using the similar conditions to the experiments. Comparison of the *L/D* ratio vs injection velocities between experimental and simulations data shows little overestimated values by the simulations (Fig. 7). The effect on *L/D* ratio with respect to injection velocity is not clear from the experimental values, may be due to less variation in the velocity values. However, the simulation results reveal slight decrease in dimensionless breakup length with an increase in velocity.

The qualitative behavior of a jet breakup length (represented by *L/D*) with jet velocity shows different breakup regimes as mentioned and shown by Ginsberg (1985) and Bürger et al. (1995) (Fig. 8). The several regimes include the laminar, transition, turbulent and atomization regimes and the transitions are expressed in terms of Weber number (We_a) and Reynolds number (*Re*). These breakup regimes and mechanisms are mostly found with smaller diameter jet cases and in gaseous environment. In order to get insights of the breakup regimes and study the variation in the trend of breakup length with injection velocities, the simulations are carried out using wide range of velocities. The results are represented by *L/D* ratio vs We_a, as

shown in Fig. 9. The preliminary observation illustrates that the behavior of the melt jet is qualitatively similar to that shown in Bürger et al. (1995). There are two peaks found in the *L/D* curve Between We_a=1-100. It is observed that near We_a=10, the jet fragmentation/breakup is dominated by the transverse instability (R-T type) resulting into coarse breakup. As the We_a increases, sideways stripping initiates, and after We_a=60, there is the combined effect of the stripping mechanism and coarse breakup. Further, at very high We_a, the stripping becomes severe resulting into smaller size droplets which is treated as atomization zone.

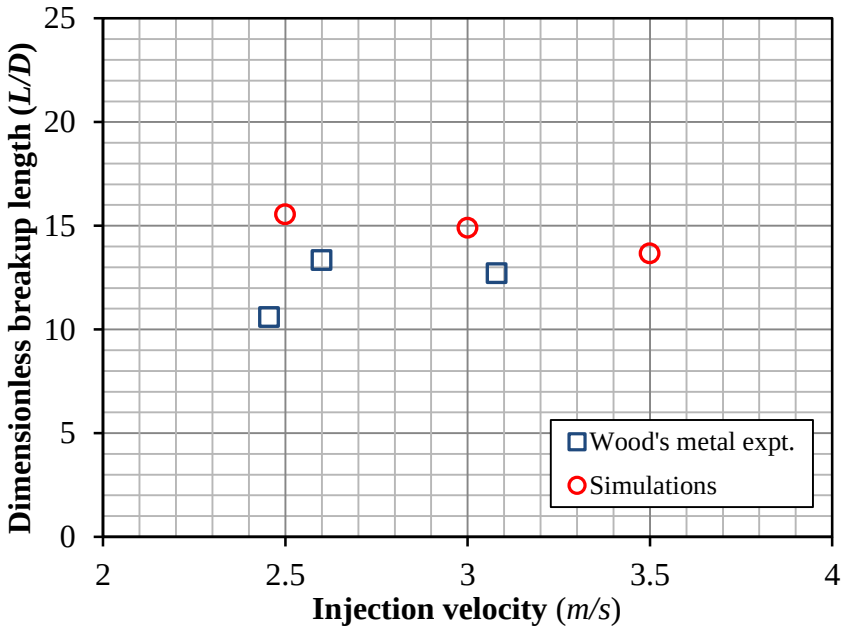

Fig. 7: Dimensionless breakup length variation with injection velocity (D_j=20 *mm*).

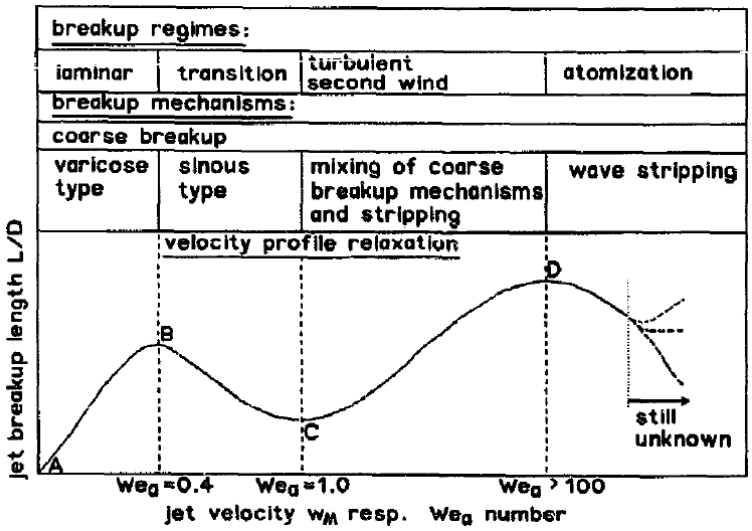

Fig. 8: Sketch of the jet breakup length curve and related breakup mechanisms (Bürger et al., 1995).

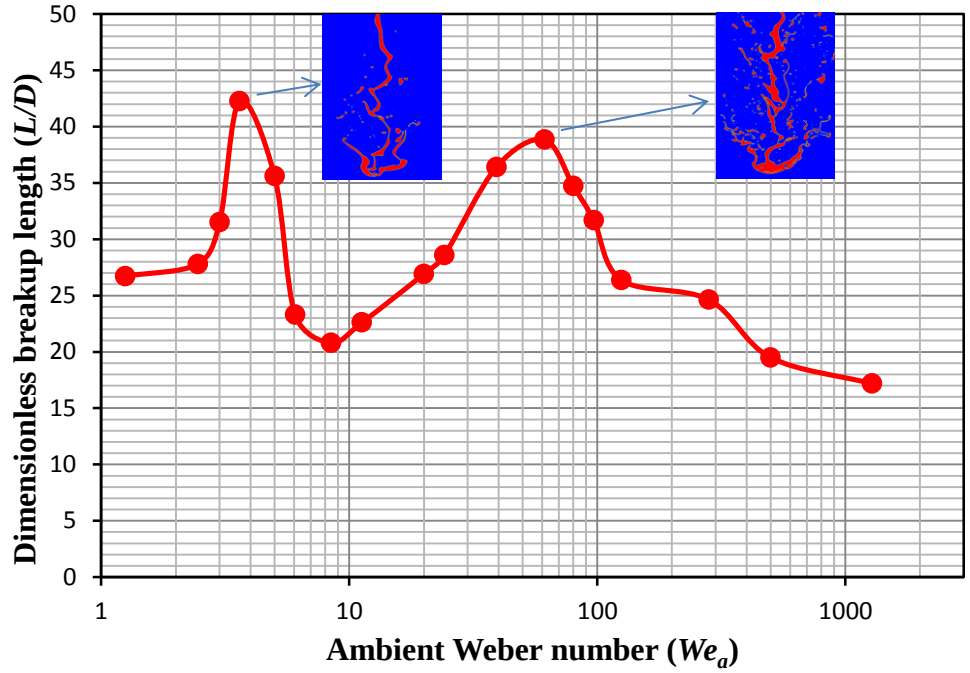

Fig. 9: Variation in the breakup length with respect to *Weber number* (D_j = 5 *mm*).

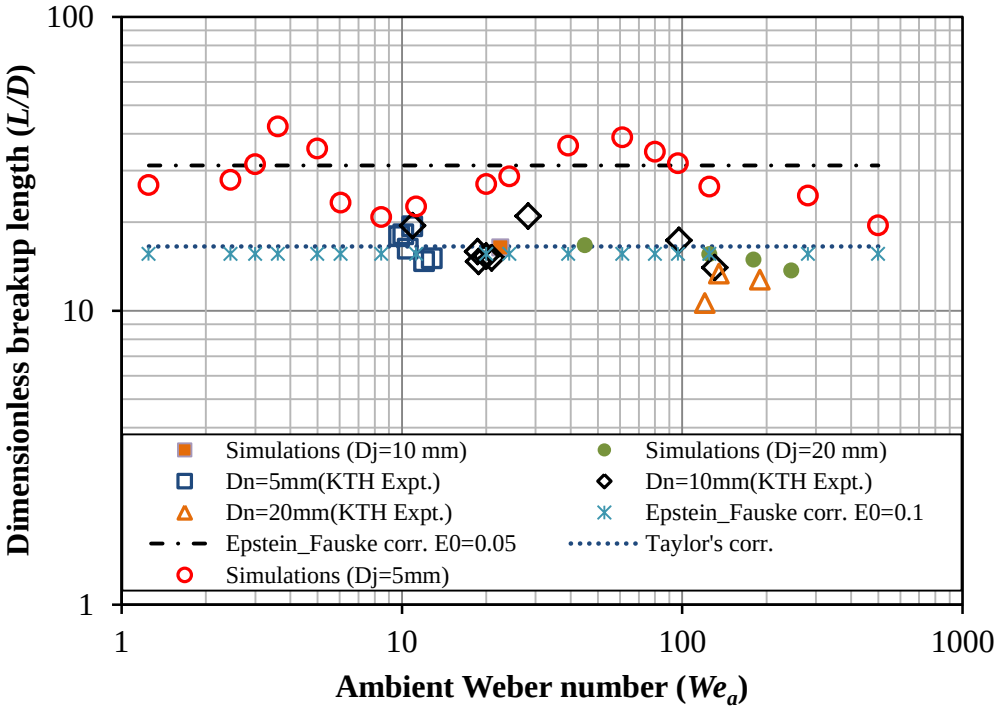

Fig. 10: Comparison of jet breakup length with correlations and experimental data.

There are theoretical developments on jet breakup study by earlier researchers based on the experimental investigations. Most of the experiments were carried out with small diameter jets in air. However, there are some experiments carried out with bigger diameter molten jets in water environment discussed by Bürger et al. (1995). Taylor (1940) proposed a correlation with proportionality coefficient determined by comparing the experimental data on the breakup of

20 *mm* jet in air and the molten jets in water (Epstein and Fauske, 2001). The correlation is given as,

$$L/D_j = 5.3\left(\frac{\rho_j}{\rho_c}\right)^{1/2} \quad (1)$$

It is found to provide a reasonable lower bound to the measured *L/D* ratio from comparison with many experimental data. Epstein and Fauske (2001) modified the correlation based on the entrainment concept which is given as,

$$L/D_j = \frac{1}{2E_0}\left(\frac{\rho_j}{\rho_c}\right)^{1/2} \quad (2)$$

where E_0 is the entrainment coefficient, putting as 0.1 in equation (2), gives Taylor's correlation. The value of E_0 between 0.05 and 0.1 in the correlation (2) stated to create the upper and lower bound for most of the *L/D* experimental data including the molten jets in water. It can also be noted the above correlations are based on the principle that the jet breakup length will not be affected by the injection velocity.

However, numbers of simulations are carried out with the same density ratio (Wood's metal), but various diameters and velocities, in order to simulate the experiments. The results are then compared with the experimental data and correlations which are represented as *L/D* versus We_a in Fig. 10. It illustrates that the simulated results of their respective experimental data shows remarkable predictions though it slightly overestimate the values in some cases. There is a significant variation in the *L/D* ratio for 5 mm jet diameter case, plotted over a wide range, but lacks the experimental data points for comparison. Although, most of the experimental and numerical data points are within the upper and lower bound of the Epstein and Fauske (2001) correlation and closer predictions with the Taylor's correlation, its application specifically to the small scale jets may be still questionable where the effect of jet diameter and injection velocity by the correlations are neglected.

Discussing other aspects, include the jets with different characteristics (diameter and velocity) but same We_a may not have same breakup length. In order to support the statement, fours cases are considered, two of which nearly equals the We_a to rest of the two cases as shown in Fig. 11. The jet with 5 *mm* diameter has 70% higher L/D ratio to that of jet with 20 *mm* jet, both of which have the same We_a. Therefore, the jet with different diameters, plotted as *L/D* versus We_a, may give a fragmentary picture and not lead to a clear conclusion.

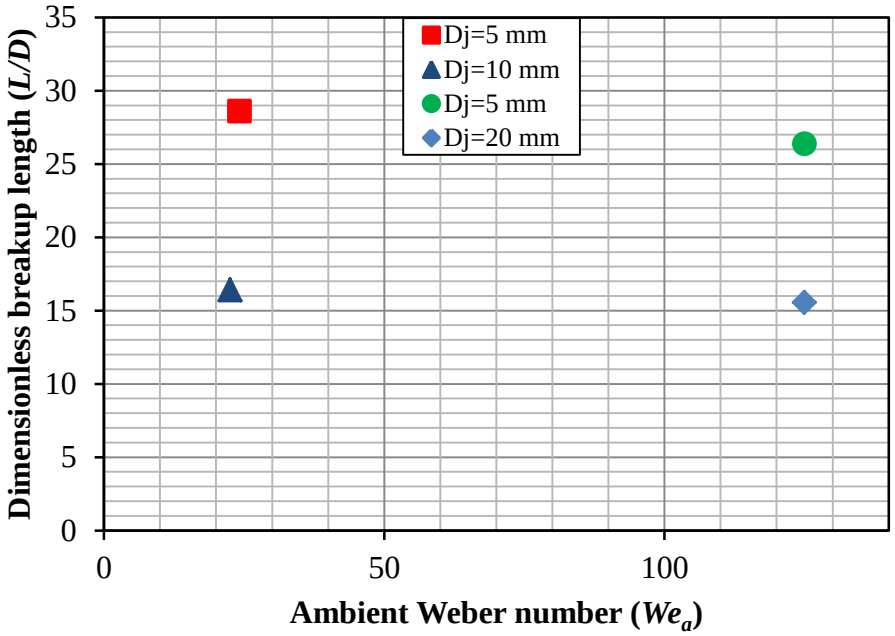

Fig. 11: Comparison of breakup length of jets with different characteristics but same We_a.

3.2.3 Effect of Density Ratio

In order to understand the effect of jet material properties on its breakup, separate effect study has been carried out changing one parameter at a time. Initially, the effect of melt density is studied. Three different density values are used in the simulations. Fig. 12 shows the variation in jet breakup length to diameter ratio (L/D) with respect to melt density ratio. It illustrates that less dense material jet is having lower L/D ratio. The melt to water density ratio in the present case is varied from 6-9 and the breakup length shows 65% enhancement for the considered range. It is seen that the Epstein and Fauske (2001) correlation primarily depends on the density ratio of a jet and surrounding fluid. Therefore, it is used for the comparison of breakup length with different density ratios. It shows that all the three points are within the upper and lower bound of the correlation.

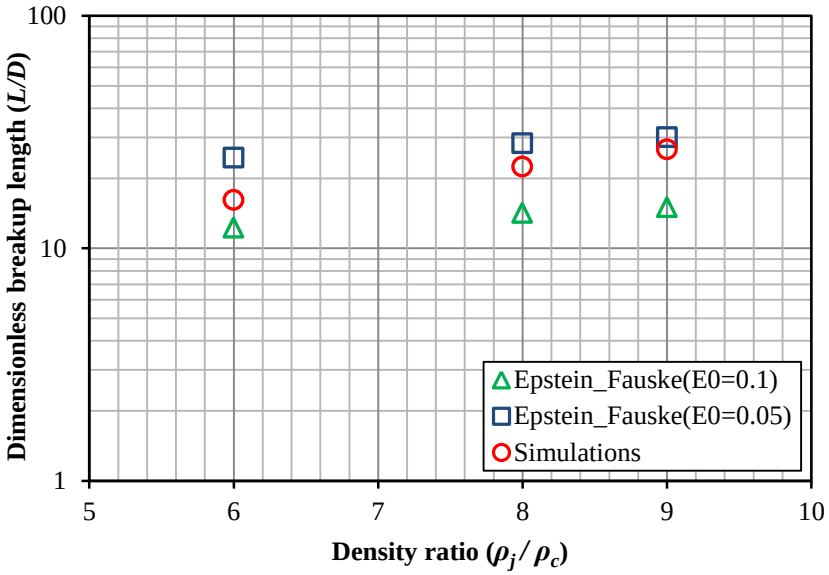

Fig. 12: Effect of jet density on breakup length (D_j=5 *mm*; V_j=1.5 *mm*).

3.2.4 Effect of Jet Dynamic Viscosity

As a next step, effect of jet dynamic viscosity on its breakup length is carried out. Three cases of viscosities are considered in this study. Fig. 13 shows the variation in non-dimensional jet breakup length (*L/D*) with respect to viscosity, which illustrates that the *L/D* ratio is slightly higher for the less viscous jet. However the effect on the jet breakup length is not linear for the considered range of values. Dinh et al. (1999) mentioned in their study from the Water-Paraffin oil experiment that jet fluid viscosity does not affect the jet instability behavior. Similarly, in the present case the effect on the jet breakup length is not significant.

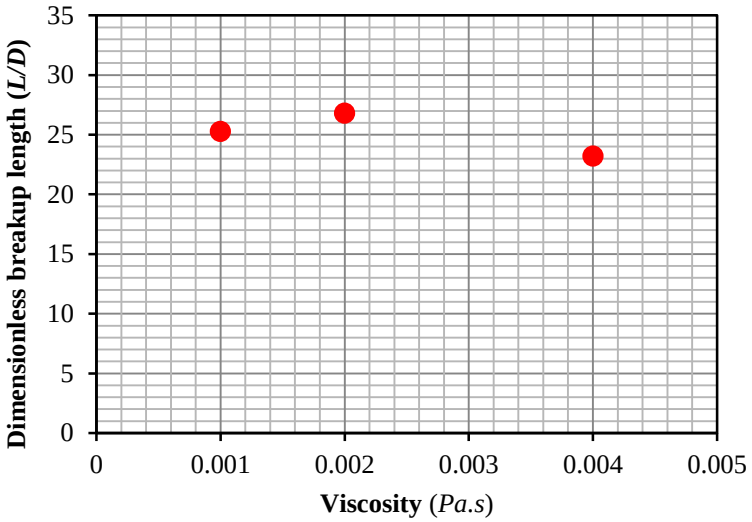

Fig. 13: Effect of jet dynamic viscosity on jet breakup length (D_j=5 *mm*; V_j=1.5 *mm*).

3.2.5 Effect of Surface Tension

The effect of surface tension in case of smaller jets can be more pronounced and therefore it has been considered in the present calculations. It is understandable that at lower surface tension, the jet surface is more prone to generate surface instabilities which cause stripping of the droplets leading to thinning of the jet. These conditions may be responsible for an early breakup of jet as compared to that having high surface tension where it can keep the jet surface intact. As stated earlier in the text, the Rayleigh-Taylor type instability occurs to the jet in the normal direction near leading edge which causes the jet breakup. Surface tension is one of the influencing factors in R-T instability theory. In linear theory, the surface tension stabilizes the perturbations shorter than a critical wavelength (Sharp, 1984), can be given in the present case as $\lambda_c = \sqrt{\sigma/g(\rho_j - \rho_c)}$. Therefore, the surface tension may have some critical value deciding the critical wavelength for the jet of a specific melt-liquid density ratio. Consequently, the higher surface tension value may grow the perturbations on the jet, leading to shorter breakup length.

Moreover, Weber number inclusively represents the effect of surface tension. Alternatively, it can be stated that the change in surface tension changes the We_a values. Fig. 14 illustrates the non-dimensional jet breakup length variation for different surface tension values. In this study, the surface tension values are not varied significantly, in order not to be away from the realistic values. It initially shows rise in the jet breakup length with increase in surface tension, till 0.8 N/m. However, the breakup length starts decreasing after achieving a peak with further increase in the surface tension values, which finally increases thereafter. The We_a ranges from 9-23 approximately for these considered surface tension values. We have earlier seen that the significant variation in the jet breakup length at lower Weber number is possible (from Fig. 9). The non-linear variation in Fig. 14 may be comprehended by the inclusive effect of surface tension in the We_a.

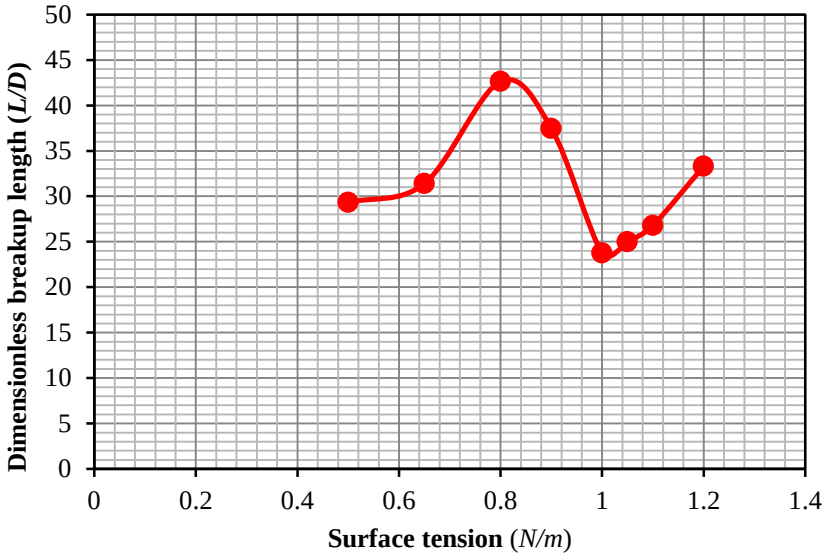

Fig. 14: Effect of surface tension on jet breakup length (D_j=5 *mm*; V_j=1.5 *mm*).

3.3 Droplet Size Distribution

The melt jet during fragmentation and breakup is surrounded by the droplets which are stripped from the jet itself. These are the fresh droplets just fragmented from the jet and still in liquid state which may participate in steam explosion if occurs. This first fragmentation is primarily due to hydrodynamic effects, though the formed droplets may undergo secondary fragmentation due to thermal effects. The size of the liquid melt droplets participating in steam explosion is instrumental in deciding its energetics.

Therefore, as a next step to the jet breakup analysis, the liquid melt droplet size distribution study has been carried out. The amount of droplets and its size may be determined by the nature of instabilities occur to the jet which depends on the characteristics of the jet such as jet velocity and diameter. Therefore, in this study, the details of the droplets fragmented from the jet are analyzed. The jet about to undergo breakup may give the most appropriate droplet distribution, due to which the jet breakup time is considered for the collection of droplet size distribution data. Since the data sets are saved at regular time intervals for each calculation case, it is easier to determine the jet breakup case and the case just before the breakup, which is used for droplet distribution analysis. It is understood that the droplets fragmented from the jet would not be spherical but may have different non-uniform shapes. Therefore, during this study, an average diameter of the non-uniform droplets is considered. Similarly for the droplets of ligament shape, length and width is measured and the diameter of equivalent sphere is used. Moreover, the droplet size measurement is carried out by calculating the distance between coordinate points from the melt volume fraction contour, for all the droplets. The precision is maintained by

magnifying the contour plots.

For the first comparison, two different diameter jets are considered. The results plotted in Fig. 15 which shows the droplet percentage with respect to their sizes. The horizontal error bar in figure is considered to show the range of the droplet sizes considered in one point. The results show the range of the fragmented droplets' diameter is from less than 1 *mm* till 5 *mm*, whereas, maximum percentage of the droplets is less than 1 *mm* which then decreases exponentially. There is no significant effect of the diameter on the droplet size distribution found from the results of these small scale jets.

Further in the droplet size distribution study, the effect of the velocity is analyzed. Three cases are considered with a range of We_a=8.5-500. Fig. 16 shows the jet with lowest velocity (1.3 *m/s*) gives wide variation in the droplet size distribution and less difference in the percentage of various size droplets. On the other hand, the jet with highest velocity (10 *m/s*) gives higher amount of very fine droplets, where almost 90% are of size less than 1 mm. For higher velocity jets, the surface instabilities (K-H type) are dominant and of shorter wavelength which leads stripping of very fine fragments. However, at lower velocities, the surface stripping is less and of comparatively longer wavelength giving bigger size stripped droplets. Moreover, at lower velocities the leading edge breakup is dominant which results into bigger size droplets.

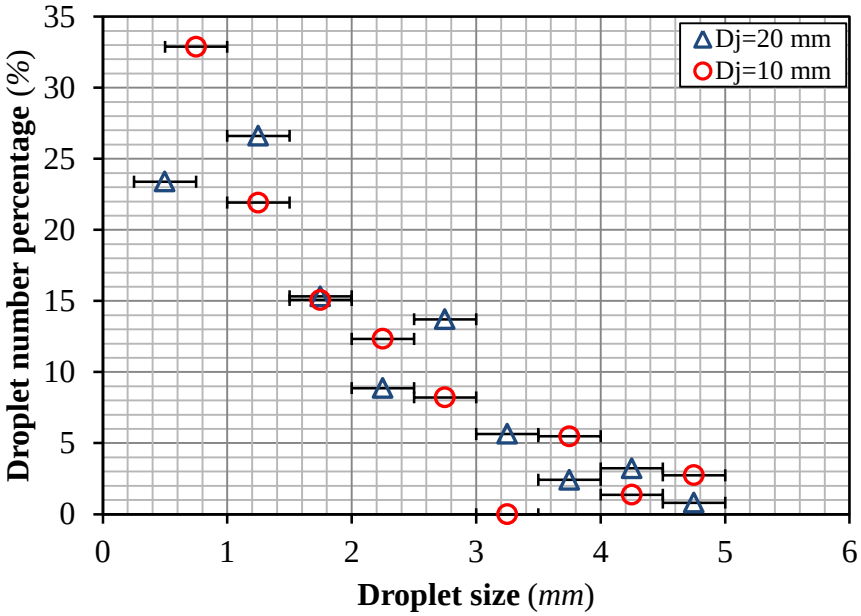

Fig. 15: Droplet size distribution for different diameter jets (V_j=1.5 *mm*).

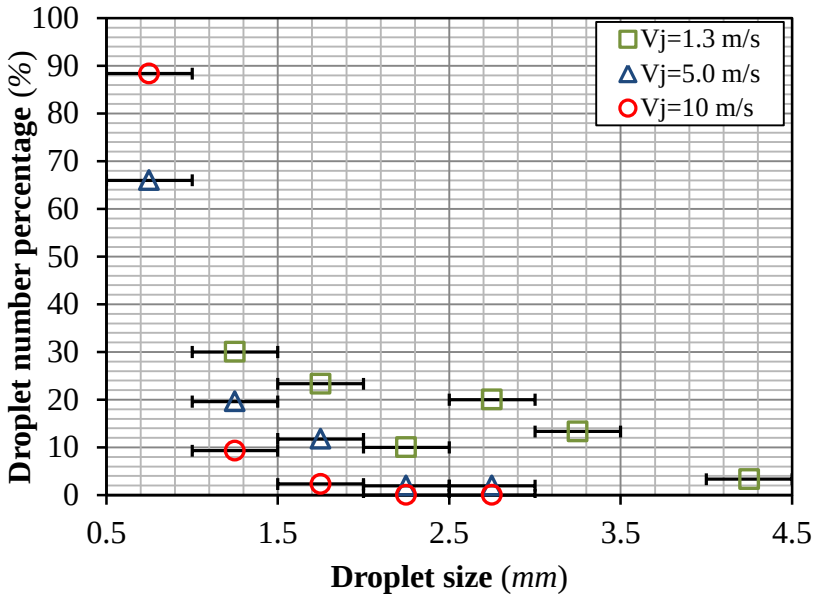

Fig. 16: Droplet size distribution for the jets with different injection velocities (D_j=5 *mm*).

4. CONCLUSIONS

A two dimensional numerical analysis of melt jet fragmentation/breakup has been carried out using the commercial CFD code, ANSYS FLUENT 14.0. The geometry and initial conditions for the simulations are taken similar to the experiment of Wood's metal molten jet breakup carried out at KTH. The study includes identification of the jet fragmentation pattern as well as the influences of Weber number and physical properties on the jet breakup length. It is demonstrated that the VOF method is capable of simulating jet fragmentation in melt coolant interactions. More conclusions are drawn from the simulation results and analyses.

- The jet breakup pattern shows that it is axisymmetric during initial deformation of the jet, which deteriorates further due to growth of instability. At lower jet injection velocities, the leading edge breakup is dominant whereas, there is the combined effect at higher velocities including the sideways stripping mechanism.
- The dynamics of jet breakup shows the jet breakup length is not constant but varies following a specific pattern. The instability on the jet surface may be responsible for the variation in the jet breakup length.
- The jet breakup length increases with an increase in the jet diameter. Generally speaking, there are less than 25% deviations between the simulated jet breakup length values and the widely spread experimental data indicating an acceptable agreement of simulation with experiment.

- The study of dimensionless jet breakup length over a wide range of Weber number shows a trend qualitatively matching to the behavior discussed in the earlier literatures.
- The dimensionless jet breakup length is found to be increasing with jet to coolant density ratio whereas, the surface tension shows the non-linear behavior for the considered range which may be comprehended by the inclusive effect of surface tension in ambient Weber number.
- The jet breakup length is slightly higher for the less viscous jet. However, the effect on the jet breakup length is not significant.
- The preliminary analysis shows no effect of the jet diameter on the size distribution of droplets fragmented from the melt jet. Whereas, the effect of jet injection velocity shows higher percentage of fine size droplets (less than 1 *mm*) due to the governing various instability mechanisms.

NOMENCLATURE

D_j	Jet diameter (*mm*)
g	Gravitational constant (m/s^2)
L	Breakup length (*m*)
Re	Reynolds number
t	Time (*s*)
V_j	Jet velocity (*m/s*)
We_a	Ambient Weber number
Δx	Mesh cell dimensions

Greek letters

ρ_j	Melt density (kg/m^3)
ρ_c	Coolant density (kg/m^3)
σ	Surface tension (*N/m*)
μ	Dynamic viscosity (*Pa.s*)
λ_c	Critical wavelength (*m*)

ACKNOWLEDGMENTS

This study is supported by the research programs of APRI8, ENSI and NKS. The discussions with the MSWI team members at KTH are gratefully acknowledged. The authors thank the staff at the NPS for their support in the discussions.

REFERENCES

ANSYS FLUENT 14.0, 2014. FLUENT 14.0 user manual. FLUENT Inc.

Bang, K. H., Kim, J. M., and Kim, D. H., "Experimental study of melt jet breakup in water," *Journal of nuclear science and technology*, Vol. 40:10, pp. 807-813, (2003).

Berg, E.V., Bürger, M., Cho, S.H., and Schatz, A., "Modelling of the breakup of melt jets in liquids for LWR safety analysis," *Nuclear engineering and design*, Vol. 149, pp. 419-429 (1993).

Brackbill, J. U., Kothe, D. B. and Zemach, C., "A continuum method for modelling surface tension," *Journal of Computational Physics*, Vol. 100, pp. 335-354, (1992).

Bürger, M., Cho, S.H., Berg, E. V., and Schatz, A., "Breakup of melt jets as pre-condition for premixing: Modeling and experimental verification," *Nuclear engineering and design*, Vol. 155, pp. 215-251, (1995).

Dinh, T. N., Bui, V. A., Nourgaliev, R. R., Green, J. A. and Sehgal, B.R., "Experimental and analytical studies of melt jet-coolant interactions: a synthesis," *Nuclear Engineering and Design*, Vol. 189, pp. 299–327, (1999).

Epstein, M., Fauske, H. K., "Applications of the turbulent entrainment assumption to immiscible gas-liquid and liquid-liquid systems," *Trans IChemE*, Vol. 79 (Part A), pp. 453-462, (2001).

Ginsberg, T., "Liquid jet breakup characterization with application to melt-water mixing," *ANS Proc. National Heat Transfer Conf.*, Denver, CO., (1985).

Mahaffy, J., "Development of best practice guidelines for CFD in nuclear reactor safety," *Nuclear Engineering and Technology*, Vol. 42, pp. 377–381, (2010).

Manickam, L., Thakre, S., Ma, W. and Bechta, S., "Simultaneous visual acquisition of melt jet breakup in water by high speed videography and radiography," Proc. of NUTHOS10, Okinawa, Japan, December 14-18, (2014).

Matsuo, E., Abe, Y., Chitose, K., Koyama, K. and Itoh, K., "Study on jet breakup behavior at core disruptive accident for fast breeder reactor," *Nuclear Engineering and Design*, Vol. 238, pp. 1996–2004, (2008).

Nishimura, S., Yamaguchi, T. and Ueda, N., "A study of the relation between thermal interaction and the fragmentation through simulant fuel coolant interaction tests," *7th*

international conference on nuclear engineering (ICONE7), Tokyo, Japan, April 19-23, (1999).

Sharp, D. H., "An overview of Rayleigh-Taylor instability," *Physica D: Nonlinear Phenomena*, Vol. 12(1), pp. 3-18, (1984).

Spencer, B. W., Gabor, J. D. and Cassulo, J. C., "Effect of boiling regime on melt stream breakup in water," *4th Miami international symposium on multi-phase transport and particulate phenomena*, Miami beach, FL, December 15-17, (1986).

Thakre, S., Li, L. and Ma, W., "A numerical analysis on hydrodynamic deformation of molten droplets in a water pool", *Annals of Nuclear Energy*, Vol. 53, pp. 228-237, (2013).

Thakre, S. and Ma, W., "3D simulations of the hydrodynamic deformation of melt droplets in a water pool", *Annals of Nuclear Energy*, Vol. 75, pp. 123-131, (2015).

Wang, S.K., Blomquist, C.A. and Spencer, B.W., "Modelling of thermal and hydrodynamic aspects of molten jet/water interaction," *ANS Prof. 26th National Heat Transfer Conf., Philadelphia, PA,* Vol. 4, pp. 225-232, (1989).